Targeting CCR2$^+$ Monocytes for Treating Acute Disc Herniation in Mouse Models

Li Xiao[1], Brock J Manley[1], Eunha G Oh[1], Yi Zhang[1], Jialun Chi[1], Wendy Huang[1], Chia-Yi Kuan [2], Li Jin[1], Xudong Li [1,3]
Departments of [1]Orthopaedic Surgery, [2]Neuroscience and Center for Brain Immunology and Glia, [3]Biomedical Engineering, University of Virginia, Charlottesville, VA, USA

Presenting author email: lx4c@virginia.edu

Disclosures: LX (N), BM (N), EO (N), YZ (N), JC(N), WH(N), CK (N), LJ (N), XL (N)

INTRODUCTION: Inflammation stands as a pivotal factor in the intricate web of mechanisms contributing to intervertebral disc degeneration, a predominant source of both back and leg pain. Evident correlations have been established between inflammatory mediators within degenerated discs and the severity of degeneration. Among these mediators, inflammatory cytokines such as IL-1β, TNF-α, IL-6, IL-8, IL-12, IL-17, IFN-γ, monocyte chemoattractant protein-1 (MCP-1), and IL-4 have been identified in surgical specimens of degenerated disc tissues, suggesting their association with the progression of degeneration. This inflammatory milieu is thought to originate from both degenerated disc cells and infiltrating macrophages. Despite the known involvement of these macrophages, their precise origins and functional roles in the context of disc herniation and pain pathogenesis remain enigmatic. C-C chemokine receptor 2 (CCR2) is a monocyte specific receptor that plays a pivotal role in inflammation and immune cell trafficking. We hypothesize that the infiltration of monocytes into disc hernia sites differentiate into a diverse macrophage population and that disruption of monocytic infiltration by blocking CCR2 signaling can attenuate local inflammation and hyperalgesia following acute disc herniation (**Figure 1**).

METHODS: To test this hypothesis, we employed genetic and pharmacological approaches to block the infiltration of monocytes in a mouse model of disc herniation. Specifically, we adopted a transgenic tamoxifen-induced CCR2-CreER; R26R-EGFP (Ai6) mouse strain to trace the influx of monocytes and heterogeneous population of CCR2$^+$ monocyte-derived macrophages at disc hernia by immunostaining, FACS, and RT-PCR. We also employed a CCR2$^{RFP/RFP}$ mouse strain and a CCR2-specific antagonist PF-4136309 to study the impacts of CCR2$^+$ monocytes on local inflammatory responses, pain level, disc degeneration, and cortical bone structure by immunostaining, von Frey assay, micro-CT, and histology. Data were shown as mean ± 95% CI. Differences between groups were analyzed by one-way ANOVA followed by Holm-Šídák's multiple comparisons test or *t* test. For comparisons among groups across two fixed-effect factors, two-way ANOVA was applied. For behavior assays, multiple *t* tests were used to determine significance at each time point. A p value < 0.05 was considered statistically significant.

RESULTS SECTION: As shown in **Figure 2**, CCR2$^+$ monocytes (GFP$^+$) increased at the sites of disc hernia over postoperative day (POD) 4, 6, and 9 in CCR2-CreER; Ai6 mice. F4/80$^+$ cells increased, and meanwhile CD11b$^+$ cells trended downward (**Fig. 2B, 2C**). Co-localization analysis revealed both GFP$^+$CD11b$^+$ and GFP$^+$F4/80$^+$ constituted the majority of CD11b$^+$ and F4/80$^+$ cells at disc hernia sites (**Fig. 2D, 2E**). As exhibited in **Figure 3**, genetic depletion of CCR2 reduced infiltration of monocytes and macrophages (**Fig. 3B,** *gating strategies not shown*), alleviated ipsilateral mechanical sensitivity (**Fig. 3C**), restored loss of disc height and changes in adjacent cortical bone (**Fig. 3D, 3E**) for up to 1 month. Pharmacologically inhibiting CCR2 produced comparable results. Due to space constraints, the accompanying data on this inhibition and the histology findings from the study are not presented here.

DISCUSSION: This study delves into the perplexing landscape by investigating the monocytic infiltration orchestrated by CCR2 and its potential significance in ameliorating local inflammation and hyperalgesia post-acute disc herniation. By utilizing a multifaceted approach, encompassing genetic and pharmacological interventions, we studied the dynamics of monocyte influx, the differentiation of CCR2 monocyte-derived macrophages, and their impact on pain sensitivity and disc degeneration. The findings unveiled the pivotal role of CCR2$^+$ monocytes in instigating and perpetuating inflammation at disc herniation sites, shaping pain sensitivity and disc degeneration. Long-term effects of CCR2 depletion over extended periods (e.g. >3months) are currently under investigation.

SIGNIFICANCE/CLINICAL RELEVANCE: This study highlights a promising therapeutic strategy centered on modulating monocyte infiltration to alleviate the acute back and radicular pain triggered by disc herniation, offering potential relief to individuals suffering from this debilitating condition.

ACKNOWLEDGEMENTS: We are grateful for financial support from NIH NIAMS R01AR064792, R01AR078888, R21AR078547, R21AR082052, and North American Spine Society.

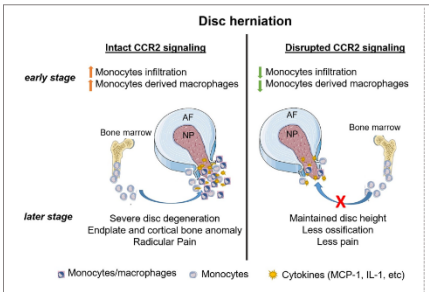

Figure 1. Proposed mechanism illustration shows that disruption of CCR2 signaling can help reduce monocyte and macrophage infiltration at early stage of disc herniation, which may subsequently retard disc degenerative change, e.g. disc height loss, and reduce radicular pain.

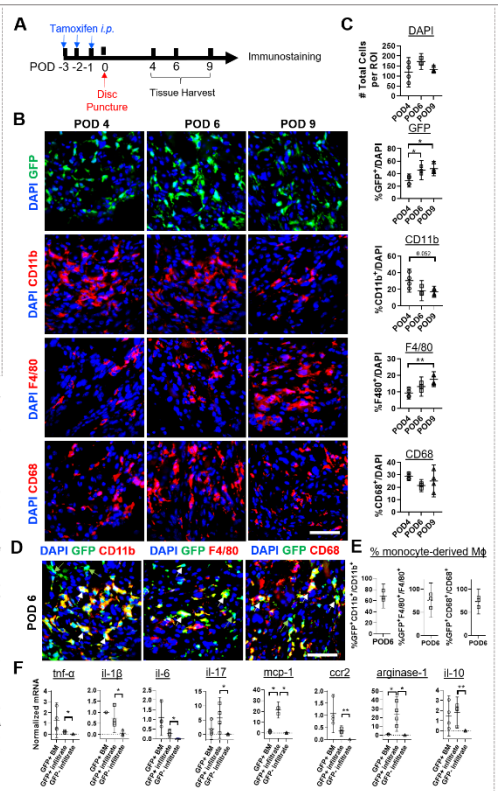

Figure 2. Detection of infiltrating CCR2 monocytes, their macrophage derivatives and cytokines at disc herniation sites in CCR2-CreER; Ai6 mice. (A) Experimental design. (B) Representative fluorescence images of GFP$^+$, CD11b$^+$, F4/80$^+$, CD68$^+$ cells on POD4, POD6, and POD9. (C) Quantification showed a stable total DAPI stained cells and an increasing GFP$^+$ cells over time; a decreasing trend of CD11b$^+$ and significant increase of F4/80$^+$ from POD 4 to POD9, and relatively stable CD68$^+$ cells. (D) Representative fluorescence images of GFP$^+$CD11b$^+$, GFP$^+$F4/80$^+$, and GFP$^+$CD68$^+$ cells on POD 6 after disc herniation. Arrows indicate co-localized cells. (E) Quantification of co-localized staining suggested the majority of CD11b$^+$, F4/80$^+$, and CD68$^+$ cells were derived from GFP$^+$ monocytes. (F) RT-PCR analysis showed that GFP$^+$ monocytes/macrophages (GFP$^+$ infiltrate) at disc hernia sites expressed significantly higher mRNA levels of *tnf-α*, *il1b*, *il6*, *il33*, *il17*, *ccr2*, *mcp-1*, *arginase-1* and *il10* compared to that of GFP$^-$ cells (GFP$^-$ infiltrate) from disc hernia sites on POD 6. GFP$^+$ and GFP$^-$ cells were sorted by FACS. Of note, mRNA levels of *mcp-1* and *arginase-1* in GFP$^+$ cells at hernia sites are higher than that of GFP$^+$ bone marrow cells. n=4 per group. For B-E, cells were counted in 10-15 sections per animal. n = 4 for POD 4 and POD 9, n = 3 for POD 6. Data combining samples from both genders was analyzed. Statistical analysis was performed one-way ANOVA followed by Holm-Šídák's multiple comparisons test. For F, significance was determined by paired *t*-test between GFP$^+$ bone marrow and GFP$^+$ infiltrate or between GFP$^+$ infiltrate and GFP$^-$ infiltrate. *p<0.05; **p<0.01; Scale bar = 50 μm

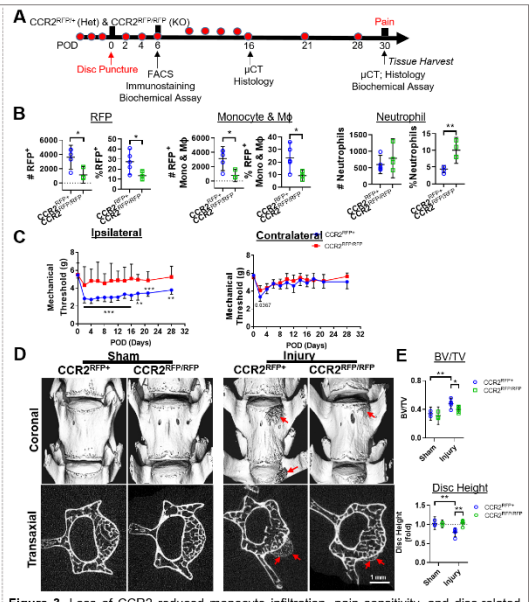

Figure 3. Loss of CCR2 reduced monocyte infiltration, pain sensitivity, and disc-related changes after herniation. (A) Workflow. (B) Quantification of flow cytometry analysis showed CCR2$^{RFP/RFP}$ mice had fewer RFP+ cells and macrophages, and more neutrophils at hernia sites compared to CCR2$^{RFP/+}$ mice. (C) CCR2$^{RFP/RFP}$ exhibited less ipsilateral pain for up to 1 month after herniation, while contralateral legs showed no significant difference. Data combining both genders was analyzed. (D) Representative μCT scan of lumbar motion segments (upper) and cross section of cortical bone (lower) one month after surgery. Red arrows: increased cortical bone roughness. Scale bar=1 mm. (E) Quantification of cortical bone volume fraction (BV/TV) of lumbar vertebrae and normalized disc height. Dotted line: normalized baseline at 1. For B, n = 4-5 mice per group by unpaired t-test. For C, n = 12-14 mice per group (both genders), multiple t-tests were performed for various time points. For E, two-way ANOVA with Šídák's test was used. *p<0.05; **p<0.01; ***p<0.001.